AD

TECHNICAL REPORT ARCCB-TR-03002

# APPLICATION OF LASER PULSE HEATING TO SIMULATE THERMOMECHANICAL DAMAGE AT GUN BORE SURFACES

PAUL J. COTE
SABRINA L. LEE
MARK E. TODARO
GAY KENDALL

FEBRUARY 2003

US ARMY ARMAMENT RESEARCH,
DEVELOPMENT AND ENGINEERING CENTER
Close Combat Armaments Center
Benét Laboratories
Watervliet, NY 12189-4000

## DISCLAIMER

The findings in this report are not to be construed as an official Department of the Army position unless so designated by other authorized documents.

The use of trade name(s) and/or manufacturer(s) does not constitute an official endorsement or approval.

## DESTRUCTION NOTICE

For classified documents, follow the procedures in DoD 5200.22-M, Industrial Security Manual, Section II-19, or DoD 5200.1-R, Information Security Program Regulation, Chapter IX.

For unclassified, limited documents, destroy by any method that will prevent disclosure of contents or reconstruction of the document.

For unclassified, unlimited documents, destroy when the report is no longer needed. Do not return it to the originator.

# REPORT DOCUMENTATION PAGE

*Form Approved*
*OMB No. 0704-0188*



| 1. AGENCY USE ONLY (*Leave Blank*) | 2. REPORT DATE | 3. REPORT TYPE AND DATES COVERED |
|---|---|---|
| | February 2003 | Final |

4. TITLE AND SUBTITLE
APPLICATION OF LASER PULSE HEATING TO SIMULATE THERMOMECHANICAL DAMAGE AT GUN BORE SURFACES

5. FUNDING NUMBERS
AMCMS No. 6111.01.91A1.1

6. AUTHORS
Paul J. Cote, Sabrina L. Lee, Mark E. Todaro, and Gay Kendall

7. PERFORMING ORGANIZATION NAME(S) AND ADDRESS(ES)
U.S. Army ARDEC
Benet Laboratories, AMSTA-AR-CCB-O
Watervliet, NY 12189-4000

8. PERFORMING ORGANIZATION REPORT NUMBER
ARCCB-TR-03002

9. SPONSORING / MONITORING AGENCY NAME(S) AND ADDRESS(ES)
U.S. Army ARDEC
Close Combat Armaments Center
Picatinny Arsenal, NJ 07806-5000

10. SPONSORING / MONITORING AGENCY REPORT NUMBER

11. SUPPLEMENTARY NOTES
Presented at Gun Tubes Conference 2002, Keble College, Oxford, UK, 15-18 September 2002.
Published in proceedings of the conference and *ASME Journal of Pressure Vessel Technology.*

12a. DISTRIBUTION / AVAILABILITY STATEMENT
Approved for public release; distribution unlimited.

12b. DISTRIBUTION CODE

13. ABSTRACT *(Maximum 200 words)*
Laser pulse heating experiments were performed to provide insights into the thermomechanical damage effects that occur at the surface of coated and uncoated gun steel under cyclic rapid heating and cooling. These effects include generation of a heat-affected zone severe plastic deformation, crack blunting, cavitation, fracture initiation, and generation of residual stresses. In addition, several of the deformation effects observed in the heat-affected zone indicate superplasticity. The results are compared with data from surfaces exposed to several different firing conditions to provide a basis for analyzing the specific role of the various degradation mechanisms. Supporting information is provided from x-ray diffraction measurement of residual stresses in the steel heat-affected zones produced in a firing environment. The measured compressive stresses are explained using dilatometry data and are shown to be consistent with the observed damage processes.

14. SUBJECT TERMS
Laser Pulse Heating, Thermomechanical Damage, Crack Blunting, Cavitation, Nanocrystallinity, Superplasticity

15. NUMBER OF PAGES
20

16. PRICE CODE

| 17. SECURITY CLASSIFICATION OF REPORT | 18. SECURITY CLASSIFICATION OF THIS PAGE | 19. SECURITY CLASSIFICATION OF ABSTRACT | 20. LIMITATION OF ABSTRACT |
|---|---|---|---|
| UNCLASSIFIED | UNCLASSIFIED | UNCLASSIFIED | UL |

NSN 7540-01-280-5500

Standard Form 298 (Rev. 2-89)
Prescribed by ANSI Std. Z39-1
298-102

## TABLE OF CONTENTS



### TABLES



### LIST OF ILLUSTRATIONS

## INTRODUCTION

Currently, many details of the erosion process on gun bore surfaces remain poorly understood. The major contributors to erosion include:

- Thermal effects
- Chemical attack by propellant gases
- Mechanical wear from projectile passage
- Mechanical loading from gas pressurization

Gun bore surfaces are typically subjected to short (5- to 10-ms) pulses of high thermal energy during firing of a round. Included among the deleterious thermal effects are melting, metallurgical transformations, thermal and transformational stresses, and surface cracking.

Bore surfaces are often electroplated with high-contractile (HC) chromium to improve resistance to erosion. The terms high-contractile and low-contractile (LC) refer to the differences in contraction during deposition and the subsequent 200°C annealing to drive out codeposited hydrogen. Because of the difference in contraction, LC chromium is uncracked prior to firing while HC chromium has a high density of embedded and surface cracks even before firing. The LC chromium coatings were developed to exploit benefits of coatings with lower crack densities. Although LC chromium cracks during firing, it remains significantly less cracked than HC chromium after firing (refs 1,2). Current efforts are also underway to develop such alternatives to chromium as magnetron-sputtered coatings.

There is extensive experience with gun bore protective coatings, including HC and LC chromium (refs 1,3,4). The most detailed compilation of this experience remains the 1946 National Defense Research Committee Report, "Hypervelocity Guns and the Control of Gun Erosion" (ref 1). X-ray diffraction studies of HC and LC chromium have also been reported (refs 5,6).

A recent survey study of chemical attack initiation in HC and LC chromium plated gun bore surfaces (ref 2) showed that chemical damage to the steel substrate begins at the tips of chromium cracks with propellant gas/metal reactions. The reaction products usually appear as gray layers or gray zones in the steel. These layers are iron oxide, iron sulfide, or mixtures of the two.

Wherever there is a heat-affected zone, a white layer (appearing lighter than the surrounding etched material in micrographs) forms in the steel immediately adjacent to and beneath the gray oxide layer. This is the familiar "white layer" indicative of carburization and nitriding (ref 1).

It is difficult to assess the role of specific damage mechanisms because they are numerous and act simultaneously on the gun bore surface during firing. In prior work, laser pulse heating was investigated (refs 7,8) to assess its ability to duplicate the essential thermal cycle effects on

uncoated and chromium-coated gun steel and to determine the effects of cyclic thermal pulsing alone (e.g., without firing pressure).

The present study compares laser pulsing results with vented combustor tests that were performed at low propellant gas pressures to more closely approximate the laser test conditions (1 atm). The data are also compared with gun firing results. The aim is to gain fresh insights into thermomechanical damage mechanisms, such as thermal fatigue and fracture initiation from thermal cycling.

A crucial parameter in determining fracture initiation is the residual stress in the heat-affected zone. The x-ray diffraction method was used to measure the residual stress in the heat-affected zone in a vented combustor specimen and in several available gun tube sections where firing produced a heat-affected zone. Dilatometry results and hot hardness data on gun steel are used to explain many of the key observations in terms of the austenite-to-martensite phase transformation.

The primary conclusions of the present study are that the compressive stress in the heat-affected zone plays a major role in controlling erosion damage initiation at the coating/steel interface and that firing pressure and sliding damage are significant factors that augment thermal fatigue damage. Delayed fracture from high-temperature hydrogen charging is another possible contributor to fracture initiation (ref 9) in areas outside the heat-affected zone.

## EXPERIMENTAL METHODS

### Specimens

All steel specimens and substrates were ASTM A723 steel (gun steel) in the quenched and tempered state, with a nominal yield strength of 1.1 GPa (160 Ksi). Uncoated gun steel was tested with laser pulse heating and vented combustor firing.

High-contractile chromium coatings were electrodeposited on gun steel substrates and annealed at 200°C for two hours to drive out codeposited hydrogen. The coatings were approximately 100-μm thick. These were tested with laser pulse heating and vented combustor firing. Chromium coatings sputtered onto gun steel substrates were also tested with laser pulse heating.

The vented combustor specimens in the present experiments were cut into halves axially by electrodischarge machining (EDM) to allow testing of multiple specimens. The two halves were inserted together into a sleeve during the test. All specimens were annealed to relieve any hydrogen charging from EDM and electroplating.

A planar sputtering facility equipped with a 50-mm Torus gun was used to provide an approximately 100-μm sputtered chromium coating on gun steel.

X-ray diffraction measurements of residual stress were performed on the following:

- Uncoated gun steel that had experienced vented combustor firing
- An uncracked surface of a 120-mm gun bore that had fired 39 high-temperature rounds
- An eroded surface of a 45-mm gun bore that had fired 20 high-temperature rounds with no cracking

Laser Pulse Heating

In the laser pulse heating experiment, radiation of wavelength 1064-nm from a neodymium-doped yttrium aluminum garnet (Nd:YAG) laser was delivered to the test specimen surface. The pulse duration was 5-ms (full width at half maximum). Lenses focused the light from the laser rod into a 10-m coiled length of all-silica optical fiber with core diameter of 600-μm, cladding diameter of 720-μm, and numerical aperture of 0.20. An optical fiber was used both for convenience and for assurance of a uniform distribution of energy at the specimen surface. Lenses at the output of the fiber projected a magnified image of the end face of the optical fiber onto the specimen surface. The spatial distribution of energy at the specimen surface was approximately uniform over a two- to three-millimeter diameter circular spot. Since the depth of the high temperatures and high thermal gradients was typically less than 0.2-mm, the heat flow for most of the heated area was approximately one-dimensional and normal to the surface, as it would be on an actual gun bore surface.

A significant portion of the laser energy is reflected rather than absorbed, depending on surface roughness and oxidation, both of which can change during heating. Therefore, the absorbed energy was measured calorimetrically, using a thermocouple spot-welded to the opposite face of the specimen to measure the specimen's overall temperature rise (refs 7,8). The need to measure the overall temperature rise limits the size of the specimen. The specimens were approximately 6×6-$mm^2$ and 2.5-mm thick. All pulse energy values quoted are for energy absorbed rather than incident. An absorbed energy density of up to 1 $J/mm^2$ would be typical for conventional high-temperature propellants.

Vented Combustor

The vented combustor consists of a combustion chamber with an attached nozzle of length 4.5-cm and orifice diameter 2-cm. A burst disk seals the output of the nozzle. Standard 155-mm propellant is ignited in the chamber and pressure builds up until the burst disk breaks, allowing the propellant gases to flow through the nozzle. The thickness of the burst disk determines the maximum pressure reached in the chamber. The region of the nozzle experiencing high-speed gas flow is the test area.

Two nozzles were tested: one of gun steel coated with HC chromium and the other of uncoated gun steel. Both nozzles were subjected to 20 firings at maximum chamber pressure of 85 MPa (15 Ksi). This pressure was empirically selected to produce chromium damage comparable to that seen in eroded regions of gun tubes. The duration of the vented combustor events was approximately 15-ms. Further test details are provided in Reference 10.

X-Ray Diffraction Stress Measurement

X-ray diffraction measurements of residual stress were performed on the uncoated vented combustor specimen and the 120-mm and 45-mm gun bore surfaces described earlier. The crack density on the vented combustor specimen was sufficiently low (on the order of 1/cm) to permit valid x-ray measurements at several locations. For all specimens, areas adjacent to the x-ray test locations were examined metallographically to confirm the presence of a heat-affected zone at the surface.

## RESULTS

Laser Pulse Heating

Figures 1 and 2 show some of the effects of laser pulse heating of gun steel coated with HC chromium. Twenty pulses of approximately 1 J/mm$^2$ were applied. The crack damage is confined to the heat-affected zone because of the limited number of heating cycles in these tests. Figure 1 was etched to bring out the interdiffusion zone at the chromium/steel interface. As discussed in Reference 7, such interdiffusion has been associated with interface degradation by the development of Kirkendall porosity.

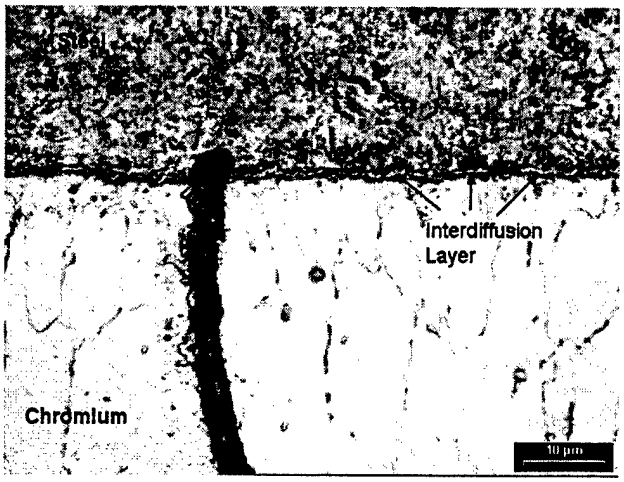


Figure 1. Typical example of crack blunting effect observed after 20 laser pulses on chromium plated gun steel specimens. Note the parallel alignment of the chromium crack faces which generally accompanies the blunting process. Such features are also commonly observed in fired gun tubes.

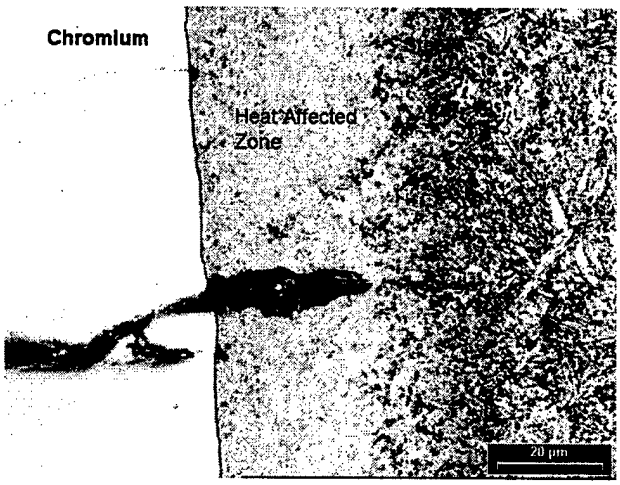


Figure 2. An example of one of the farthest progressions of blunt cracks after 20 laser pulses of a chromium plated specimen. An example of damage initiation in the steel at the tip of a fine chromium crack is seen in the upper part of the figure.

Figure 2 shows one of the largest cracks seen in the heat-affected zone due to application of 20 laser pulses. As seen here and in numerous similar experiments, such cracks generally exhibit pronounced blunting despite the high hardness and accompanying low fracture toughness of the heat-affected zone. The large crack in Figure 2 actually exhibits significant cavitation.

Figures 3 and 4 show several of the larger cavitations that occurred in laser pulse heated specimens that were coated with sputtered chromium. Twenty pulses of approximately 1 J/mm$^2$ were applied. The asymmetry of the void observed in Figure 4 was caused by the long, thin surface inclusion visible at the chromium/steel interface. Similar surface inclusions are seen elsewhere along this interface and were probably introduced during surface grinding. The asymmetric shape of the large void in Figure 4 is due to the lack of adhesion between the inclusion and the steel, which allowed the steel to pull away from the inclusion during the cavitation process. On the other hand, the coating-to-inclusion adhesion is expected to be good because that inclusion surface was exposed to the sputter-cleaning process prior to deposition. We observe similar disbonding effects at cavitation sites in specimens where poor adhesion exists between the coating and the steel.

Another remarkable feature shown in Figures 1 through 4, and often observed in gun tubes, is the essentially constant width of each of the chromium cracks through the thickness of the coating, the crack faces being aligned parallel to each other rather than in the expected V shape. Although not shown here in its entirety, the uniformity of the crack widths extends throughout the coating. This effect indicates a loss of any significant constraint exerted on the chromium coating by the substrate steel.

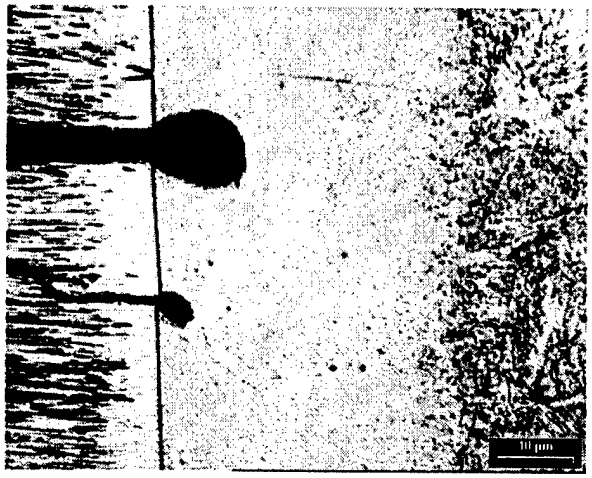

Figure 3. Examples of crack blunting in sputtered chromium specimen after 20 laser pulses. The cavitation process has extended to nearly cylindrical voids.

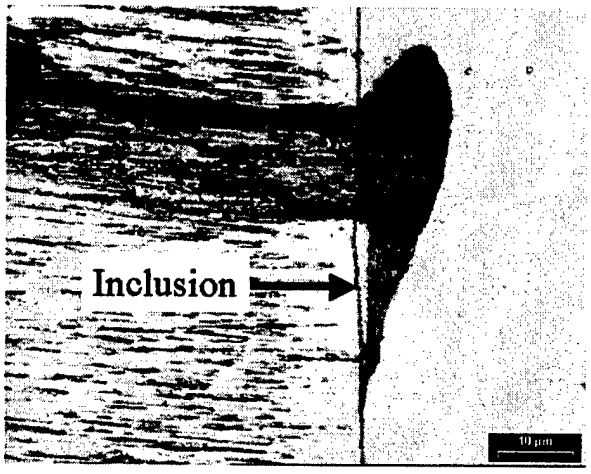


Figure 4. Example of cavitation extending into a large void under laser pulse heating of the sputtered chromium specimen. In this case an inclusion evidently enhanced the process.

Numerous laser pulse-heating experiments (with 1, 5, and 20 pulses) have previously been performed on uncoated gun steel, including experiments at pulse energies sufficient to produce melting (refs 7,8). Heat-affected zones are always formed at the energies used in the present tests. In contrast to the coated specimen results, however, no localized damage initiation in the form of cracks or cavitations has ever been observed in the heat-affected zones of laser pulsed specimens of uncoated gun steel.

Grain sizes in the heat-affected zone cannot be resolved by optical microscopy or scanning electron microscopy. Atomic force microscopy was performed on etched specimens of laser pulse heated specimens. The images indicate nanocrystalline grain sizes (typically ranging from 20- to 100-nm) in the heat-affected zones.

Vented Combustor Firing

After the 20 shots, the vented combustor sections (halves) were polished to reveal details of the cracking in the heated regions. Figures 5 and 6 show the typical crack blunting effects observed in the vented combustor nozzle coated with HC chromium. Just as for the laser pulse heating of HC and sputtered chromium, the blunting in the chromium-coated vented combustor nozzle is quite pronounced. This nozzle has a deep heat-affected zone, up to 150-μm thick, depending on location along the nozzle axis, because of the long pulse duration (approximately 15-ms). The crack widths in the chromium-coated vented combustor nozzle are clearly seen to be uniform throughout the coating, just as they are in the HC and sputtered chromium coatings that were laser pulse heated.

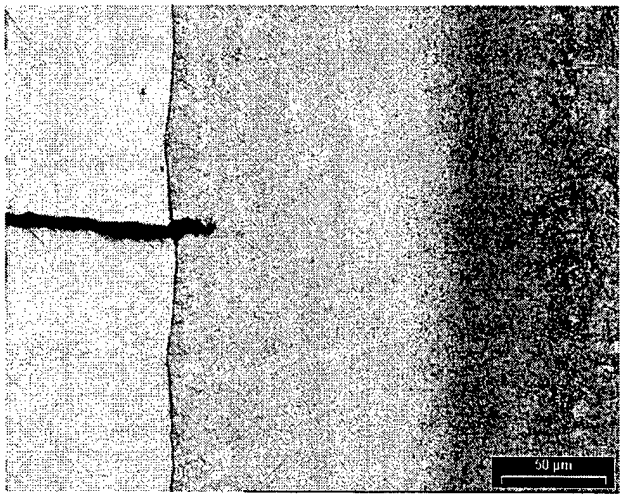


Figure 5. An example of crack blunting in the heat-affected zone of the chromium plated vented combustor nozzle.

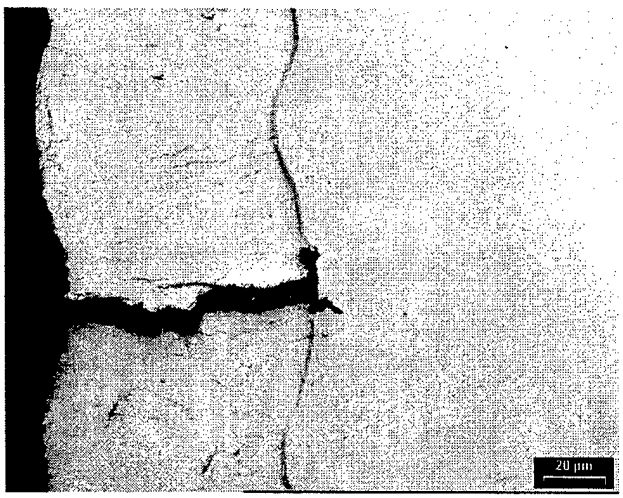


Figure 6. Another example of crack blunting in the heat-affected zone of the chromium plated vented combustor nozzle.

Figure 7 shows examples of propagation of the blunt cracks through most of the steel heat-affected zone in the chromium-coated vented combustor nozzle. The results are similar to those observed in Figure 2 for laser pulse heated HC chromium. This image was recorded from the wider flange area of the vented combustor nozzle, where the heating is less severe. The arrow indicates the approximate depth of the heat-affected zone at this location.

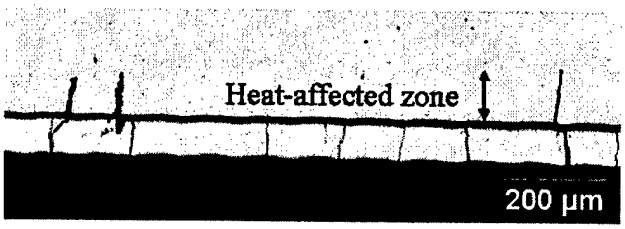


Figure 7. Examples of typical blunt crack propagation through the heat-affected zone of the chromium plated vented combustor nozzle.

For comparison, three randomly selected axial cuts were made in both the uncoated and chromium-coated vented combustor specimens, and cracks were counted on the cut surfaces after metallurgical mounting and polishing. The key results are shown in Figure 8. The most revealing result in terms of damage initiation is the observation of numerous subsurface cracks in both specimens. The numbers of fully developed cracks and subsurface cracks for the coated and uncoated specimens are given in Table 1. The "subsurface cracks" in this context, refer to cracks that exist below the heat-affected zone, but which have not actually broken through to the nozzle surface or chromium/steel interface. The arrows indicate the approximate depths of the heat-affected zones. Note the tendency for blunting and cavitation where these subsurface cracks extend into the heat-affected zone. The blunting and cavitation is more pronounced for cracks that propagate from the subsurface than for any cracks that propagate from the surface (Figure 7)

**Table 1. Number and Types of Cracks Exposed by Sectioning of Nozzles**

| Nozzle | Full Cracks | Subsurface Cracks | Total Cracks |
|---|---|---|---|
| Uncoated | 21 | 7 | 28 |
| Chromium-Coated | 16 | 6 | 22 |

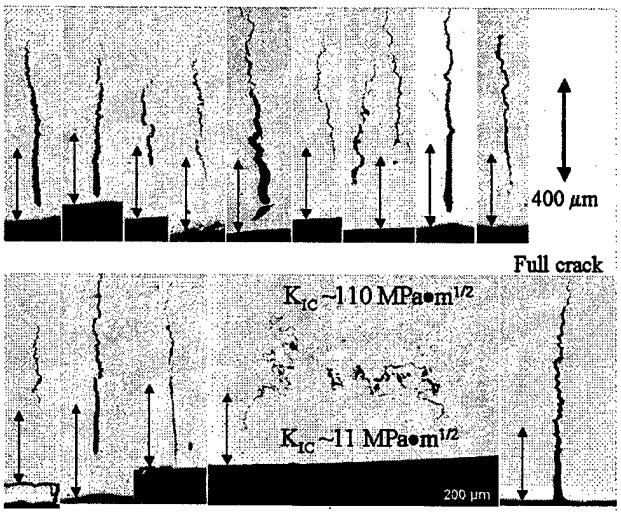


Figure 8: Collection of micrographs of subsurface cracks that formed in the chromium-coated and uncoated vented combustor nozzles. Note the initiation of cavitation in some of the examples. One figure shows multiple subsurface cracks that probably represent a flaw in the steel. Nominal values of $K_{IC}$ are labeled in the heat-affected zone and in the tempered martensite zone to underline the remarkable resistance of the brittle layer to fracture.

Figure 8 includes an example of a fully developed crack extending from the nozzle surface to well below the heat-affected zone. This crack is typical of all the fully developed cracks in both the uncoated and chromium-coated nozzles. It shows the tendency of these cracks to propagate in a relatively straight line within the heat-affected zone and to follow a meandering path along the prior austenite grain boundaries below the heat-affected zone. Similarly, subsurface cracks tend to follow the prior austenite grain boundaries.

Examination of the nozzle surface immediately above the subsurface cracks reveals unusual surface upheavals and depressions that trace the path of the subsurface cracks along the specimen surface. This is true both for the uncoated nozzle and the chromium-coated nozzle where the coating had been eroded away. These tracks often extend several millimeters in relatively straight lines along the surface. The upheavals and depressions form as a direct result of the cavitation process beneath the surface and necessarily reflect a high degree of plastic flow. On the chromium-coated nozzle, the fact that the subsurface cracks propagate in straight lines that do not follow the original randomly oriented chromium cracks is further evidence that the cracks nucleate and propagate beneath the surface rather than by propagation of the chromium cracks into the steel substrate.

The uncoated nozzle exhibits either subsurface cracks or fully developed cracks. There are no surface crack initiation sites (i.e., no short cracks that initiate at the surface and penetrate only a short way into the heat-affected zone). Thus, for the uncoated nozzle, there is no evidence of any crack initiation at the surface. All crack initiation evidently occurred below the surface.

In contrast, for the chromium-coated nozzle, there were numerous damage initiation sites in the steel at the chromium/steel interface. In fact, most of the chromium cracks had damage initiation in the steel at the chromium/steel interface as indicated in Figures 6 and 7. Note that the total number of fully developed cracks in the chromium-coated nozzle is actually smaller than in the uncoated nozzle (16 versus 21). This is unexpected, given the preexisting chromium cracks and numerous damage initiation sites in the steel at the chromium crack tips and the absence of surface crack initiation in the uncoated nozzle.

The apparent discrepancy can be explained by assuming that subsurface cracking is the primary crack mechanism and is caused by hydrogen charging. Since chromium is a hydrogen barrier, it will serve to delay hydrogen charging in the coated specimen until its effectiveness is reduced by the development of coating cracks during firing.

X-Ray Diffraction Stress Measurement

Table 2 lists the x-ray diffraction measurements of residual stress in the heat-affected zone of three representative specimens. The stress values are all compressive, in the 200 to 300 MPa (30 to 40 Ksi) range. Compressive stresses are generally observed for transformation-hardened steel surfaces. For example, similar compressive stress values are reported for laser-hardened surfaces (ref 11).

**Table 2. X-Ray Diffraction Stress Measurements**

| Specimen | Stress (MPa, Ksi) | Stress Error (MPa) |
|---|---|---|
| 120-mm Gun Tube | -277, -40 | ±3.5 |
| Unplated Vented Combustor | -212, -31 | ±5.0 |
| 45-mm Gun Tube | -239, -35 | ±4.4 |

Figure 9 is a dilatometer result for a gun steel specimen, illustrating the dilation (strain versus temperature) due to thermal expansion and the austenite and martensite phase transformations. These data will be used in the discussion section to explain some of the features exhibited in the heat-affected zone, including crack blunting, cavitation, and residual stress.

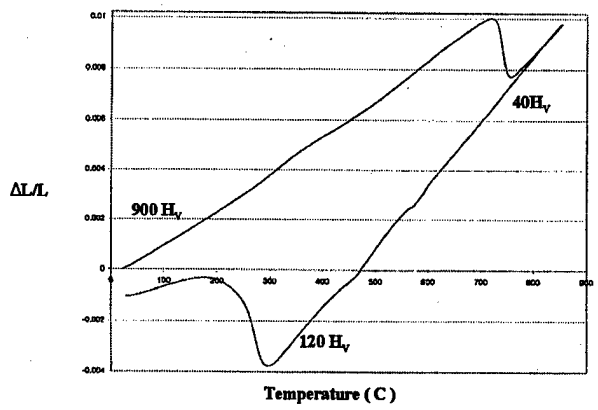


Figure 9. Dilatometer results showing strains during one complete thermal cycle.

Figure 9 shows a thermal expansion on heating followed by a contraction during the austenite phase transformation near 750°C. On cooling, the contraction is greater in the austenite phase because of the higher coefficient. The contraction is interrupted by the martensite expansion near 280°C. Also labeled are our measured values of Vickers hardness corresponding to the indicated location on the thermal cycle.

Unique Crack Pattern on Rifled Bore Surfaces

Figure 10 is an optical image of an eroded land on a rifled 155-mm gun bore. Unlike smoothbore tank gun projectiles, which use nylon "bore rider," the 155-mm projectiles use a metal rotating band that engages the bore rifling. The surface of this gun, both lands and grooves, was originally electroplated with a 100-μm thick coating of HC chromium, which eroded away after 476 rounds at high firing rates. Figure 10 is shown because it is typical of rifled 155-mm gun surfaces (ref 2). The network of cracks form a "brickwork" pattern with the long dimension of the bricks oriented perpendicular to the sliding wear direction. The chromium coating adjacent to the eroded area has this same brickwork pattern in addition to the smaller-featured, random heat-checking pattern that normally appears on HC chromium. As with subsurface cracks, the crack pattern shown here cannot form from propagation of the randomly oriented chromium cracks into the steel. The metal rotating band is evidently responsible for the unique crack morphology of rifled 155-mm surfaces.

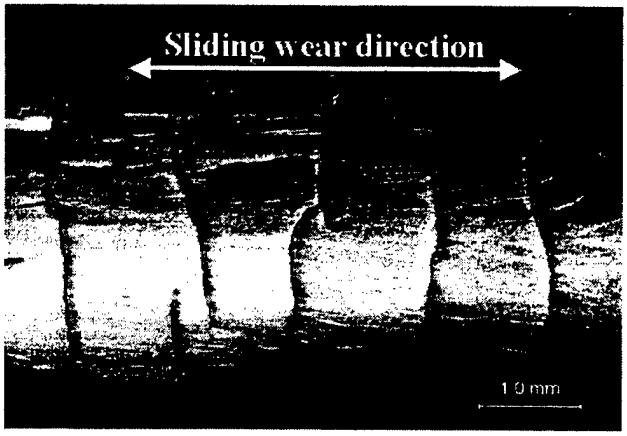


Figure 10. Crack pattern along one of the lands of a 155-mm gun specimen. The major cracks are aligned across the wear marks that form as a result of sliding contact with the metal rotating band.

## DISCUSSION

First, consider the origin of compressive residual stress in the heat-affected zone in terms of the dilatation data in Figure 9. Initially, before any thermal cycling due to firing or laser pulsing, the steel is tempered martensite. After the first cycle, the steel near the surface has quenched to untempered martensite and will tend to remain untempered martensite during subsequent rapid heating up to the contraction and transformation to austenite at 700 to 750°C. At low temperatures, the yield strength of untempered martensite corresponding to the indicated Vickers hardness of 900 is approximately 1.6 GPa (230 Ksi.). On heating above the austenite transformation, the hardness drops to Vickers hardness of 40 allowing the steel to yield dramatically, producing an essentially unstressed state.

After heating ceases, the steel near the surface rapidly cools, or self-quenches, due to heat conduction into the bulk. The thermal expansion coefficient for austenite ($\sim 25\times10^{-6}$/°C) is considerably higher than that for martensite ($\sim 12.5\times10^{-6}$/°C). The rapid contraction from an essentially unstressed high-temperature condition then produces tensile stresses.

A key point, shown in Figure 9, is that upon cooling, the steel remains as low-strength austenite until transforming to high-strength, low toughness (~11 MPa•$m^{1/2}$ (10 Ksi•$in^{1/2}$)) untempered martensite. The actual yield strength of the austenite during the quench is unknown, as is the strength of the untempered martensite during rapid heating. We can assume, however, that the strength of austenite will not exceed that of the more heavily alloyed austenitic stainless steels, so, in this range, the maximum yield strength is assumed to be ~140 MPa (20 Ksi), consistent with the measured hot Vickers hardness of 120 and typical strengths of low alloy stainless steels. Given such low strengths during the quench, large tensile yielding will occur and the maximum possible tensile stress should be correspondingly low, limited roughly to the assumed 140 MPa (20 Ksi) yield strength. Thus, the dominant contribution to the residual stress in the heat-affected zone must be the volume expansion accompanying the subsequent transformation to high-strength martensite.

If one assumes, unrealistically, that martensite plates form with no yielding of the surrounding austenite, one can estimate from the indicated strain of ~0.4%, an upper limit of 1.2 GPa (170 Ksi) for the resulting compressive residual stress. At the other extreme, allowing for the fact that the martensite plates form within a low-strength austenite matrix, the residual compressive stress could conceivably be as low as the yield strength of austenite, on the order of 140 MPa (20 Ksi). The measured residual stresses, in fact, fall within these limits, deduced from the dilatometry data. The fact that the measured values are near the lower limit suggests that the yielding of the soft austenite plays a dominant role in limiting the stress generated during martensite formation.

Next, consider the phenomenon of crack blunting and cavitation in laser pulse heating (Figures 2, 3, and 4) and indications of cavitation in low-pressure vented combustor firing (Figure 8). These effects cannot occur when the heat-affected zone is in the fully hardened, brittle untempered martensite state. In light of the phase transformation and yielding processes discussed earlier, the observed blunting and cavitation must be produced during the rapid cooling stage, when substantial tensile yielding occurs in the soft austenite.

Figure 11 is a schematic of the main features responsible for the cavitation induced at the coating crack tips by laser pulse heating, when no external pressure is present (P = 0). In that case, the constraint of the cold substrate prevents strains in the plane of the surface so that all strains, elastic and plastic, in the heated surface layers are vertical, or normal, to the surface. At high temperature, the chromium plate and heated steel, including the heat-affected zone, are compressed sufficiently to cause vertical metal flow, until most of the stresses are relieved in the chromium and heat-affected zone. Upon quenching from this state, the steel in the heat-affected zone will tend to contract roughly three times faster than the chromium plate above it, producing a condition of hydrostatic tension that leads to cavitation at initiation sites provided by the chromium cracks.

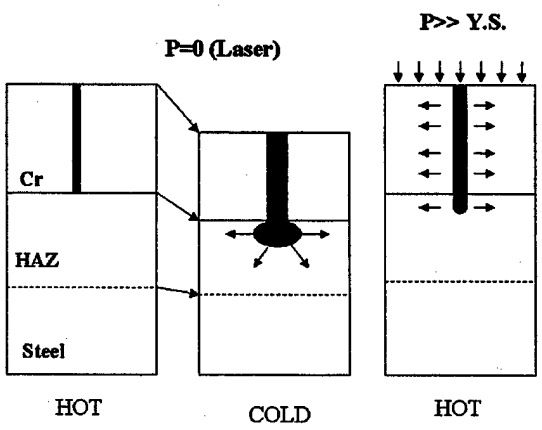


Figure 11. Schematic of cavitation process in the laser pulse heating experiments. Also illustrated is the effect of pressure in suppressing the cavitation process.

Also shown in Figure 11 is the expected influence of pressure on the cavitation process. As long as the external pressure exceeds the yield strength, i.e., the approximate magnitude of the hydrostatic tensile stress from the differential thermal contraction, cavitation should be suppressed. This is consistent with the fact that cavitation is generally not observed in gun tubes where propellant gas pressure is present during the thermal cycle. In this case, pressure will act on the crack faces to drive the crack via ductile fracture. Pressure-driven ductile fracture is expected to be the dominant damage mechanism in the heat-affected zone at elevated temperatures in gun firing because the firing pressures greatly exceed the thermal stresses, which are limited by the yield strength.

The magnitudes of the plastic strains that occurred at the surfaces of the cavities in Figures 3 and 4 are unusually large. If one assumes, conservatively, that the cavities in these figures start flat with a width equal to the chromium crack widths, then we are observing strains in 500 to 800% range, indicative of high strain rate superplasticity. The essential conditions for high rate superplasticity are small grain size and high temperature (greater than 0.5 melting point) (ref 12). Both are present in the heat-affected zone since the grain size is submicron. Given that superplasticity is likely to be present in the heat-affected zone, the flow stresses will actually be substantially less than the yield strengths assumed in the discussion of the processes associated with Figure 9.

Cavitation upon deformation is a characteristic of superplastic materials. It is also known that application of pressure in excess of the flow stress will suppress cavitation (ref 13). This is consistent with our interpretation of the role of propellant gas pressure on cavitation in the heat-affected zone.

The presence of high-temperature superplasticity in the normally brittle heat-affected zone offers an explanation for the wide variety of unusually large deformations observed therein. This includes cavitation, crack blunting, loss of coating constraint by the substrate steel, and the large surface dilations associated with subsurface cracks in the vented combustor experiments.

The presence of compressive residual stress in the heat-affected zone explains a number of observations:

- The absence of cracks, surface-initiated or otherwise, in the uncoated, laser pulse heated specimens
- The absence of surface-initiated cracks in the uncoated vented combustor nozzle
- The existence, in both uncoated and coated vented combustor nozzles, of numerous lengthy subsurface cracks below the heat-affected zone that do not propagate upward completely through the heat-affected zone
- The resistance to propagation of numerous fracture initiation sites at the chromium crack tips in the laser pulse heated chromium-coated specimens (both HC chromium and sputtered chromium), in the chromium-coated vented combustor nozzle, and in fired chromium-coated gun bore surfaces (reported in Reference 7 and 8)

Because the fracture toughness of the heat-affected zone is so low, any significant tensile stress would quickly induce brittle crack growth from the coating cracks and the damage initiation sites within the steel at the coating crack tips.

Subsurface cracks in fired guns are rarely observed. They are usually considered anomalies. This difference between vented combustor and fired gun results can be attributed to the effect of the high firing pressure that will tend to rapidly drive surface or subsurface cracks through the heat-affected zone.

Regarding the possibility of hydrogen cracking, the compressive stress in the heat-affected zone prevents the delayed hydrogen cracking so that such cracking can only initiate and propagate below the heat-affected zone.

The absence of subsurface cracks in the laser pulsed specimens contrasts with the numerous subsurface cracks that occur in the vented combustor nozzles for the same number of cycles. It is likely that high-temperature hydrogen charging occurred in the vented combustor nozzles and led to the rapid development of subsurface cracks. The smaller number of cracks in the coated vented combustor specimen and the strong tendency for the subsurface cracks to propagate along the prior austenite grain boundaries supports the hydrogen interpretation. It is noted, however, that thermal fatigue can also be intergranular, so observations of intergranular fracture may not be definitive.

Any crack propagation in the laser pulse heated specimens must be due primarily to ductile fracture and/or cavitation during tensile loading in the self-quench stage. For example, corrosion fatigue is ruled out by the ductile nature of the damage and the fact that the experiments were performed in air at atmospheric pressure. Similarly, crack initiation and propagation in the heat-affected zones of the vented combustor nozzles exhibit ductile fracture and some cavitation features, the latter due to the low-pressure condition of the tests.

The above discussion of the beneficial effects of the heat-affected zone may be misleading. There are conditions where the heat-affected zone is detrimental. For example, if mechanical loading in excess of the residual stress is applied, (e.g., due to metal rotating bands or projectile balloting) the low toughness heat-affected zone will fracture readily. As another example, if one follows high-flame temperature rounds with low-flame temperature rounds, a tensile residual stress can be induced in the brittle heat-affected zone, which will tend to produce extensive fracture.

The data on the unique "brickwork" crack pattern on eroded surfaces of rifled 155-mm gun bores were included in an attempt to provide a more complete picture of the fracture initiation mechanisms in large caliber guns. The long axes of the brickwork cracks that form in the 155-mm chromium coating and propagate into the steel substrate, as shown in Figure 10, are aligned perpendicular to the wear direction of the metal rotating band. Gawne (ref 14) showed that this is characteristic of sliding wear and sliding fatigue for chromium when metal-to-metal sliding contact occurs. The same process leads to interface fatigue failure and chromium spallation.

In summary, compressive residual stress and crack blunting from superplasticity in the heat-affected zones of gun bore surfaces are beneficial features that tend to offer protection in the firing environment. In low-pressure conditions, damage initiation is from thermal fatigue, and hydrogen embrittlement is expected to be subsurface because of the protection offered by the compressive stress in the heat-affected zone. Under high-pressure firing conditions in 120-mm guns, mechanical loading from gas pressure appears to rapidly drive ductile cracks through the heat-affected zone, since subsurface cracks are generally not observed. Also absent in fired gun tubes is any indication of the cavitation seen in laser pulse heating. This is taken as another illustration that pressure plays a significant role in damage initiation in gun tubes. In 155-mm guns, the mechanical effects associated with sliding fatigue represent the dominant crack initiation mechanism.

## REFERENCES


1. Burlew, J.S., ed., "Hypervelocity Guns and the Control of Gun Erosion," Summary Technical Report of the National Defense Research Committee, Division 1, Office of Scientific Research and Development, Washington, DC, 1946.

2. Cote, P.J., and Rickard, C., "Gas-Metal Reaction Products in the Erosion of Chromium-Plated Gun Bores," *Wear*, Vol. 241, 2000, pp. 17-25.

3. Ahmad, I., "The Problem of Gun Barrel Erosion – An Overview," *Gun Propulsion Technology*, (L. Stiefel, ed.), Progress in Astronautics and Aeronautics Series, AIAA, Washington, DC, 1988, pp. 311-355.

4. Dowding, J.S., and Montgomery, J.S., eds., *Proceedings of the Sagamore Workshop on Gun Barrel Wear and Erosion*, U.S. Army Research Laboratory, Wilmington, DE. 29-31 July 1996.

5. Lee, S.L., Windover, D., and Mello, K., "Grain Orientation in Electrolytic Chromium Deposition," *Advances in X-Ray Analysis*, Vol. 41, 1998, pp. 707-717.

6. Lee, S.L., and Windover, D., "X-Ray Determination of Texture and Residual Stress in Low Contraction Electrolytic Chromium Coatings," *Proceedings of SEM Spring Conference on Experimental and Applied Mechanics*, Society for Experimental Mechanics, Bethel, CT, 1998, pp. 221-223.

7. Cote, P.J., Kendall, G., and Todaro, M.E., "Laser Pulse Heating of Gun Bore Coatings," *Surface and Coatings Technology*, Vol. 146-147, 2001, pp. 65-69.

8. Cote, P., Todaro, M., Kendall, G., and Witherell, M., "Gun Bore Erosion Mechanisms Revisited with Laser Pulse Heating," *Surface and Coatings Technology*, to be published.

9. Underwood, J., Parker, A., Cote, P., and Sopok, S., "Compressive Thermal Yielding Leading to Hydrogen Cracking in a Fired Cannon," *Transactions of the ASME*, Vol. 121, 1999, pp. 116-120.

10. Crayon, D., Fish, A.E., and Hyland, E., "Coatings Evaluation Using a Vented Combustor," *Experimental Techniques*, July/August 2002, pp. 24-27.

11. Ganev, N., Kraus, I., and Trpcevska, J., "X-Ray Measurement of Residual Stresses Induced by Laser Treatment," *Physica Status Solidi A: Applied Research*, Vol. 115, 1989, pp. K13-15.

12. Higashi, K., Okada, T., Mukai, T., and Tanimura, S., "Very High Strain Rate Superplasticity in a Mechanically Alloyed IN9052 Alloy," *Journal of Materials Science and Engineering A*, Vol. 159, 1992, pp. L1-L4.

13. Chokshi, A.H., and Mukherjee, A.K., "The Influence of Hydrostatic Pressure on Grain Boundary Sliding in Superplasticity," *Journal of Materials Science and Engineering A*, Vol. 171, 1993, pp. 47-54.

14. Gawne, D.T., "Failure of Electrodeposited Chromium Coatings on Cast Iron Substrates," *Thin Solid Films*, Vol. 118, 1993, pp. 385-393.

TECHNICAL REPORT INTERNAL DISTRIBUTION LIST

| | NO. OF COPIES |
|---|---|
| TECHNICAL LIBRARY<br>ATTN: AMSTA-AR-CCB-O | 1 |
| TECHNICAL PUBLICATIONS & EDITING SECTION<br>ATTN: AMSTA-AR-CCB-O | 3 |
| PRODUCTION PLANNING & CONTROL DIVISION<br>ATTN: AMSTA-WV-ODP-Q, BLDG. 35 | 1 |

NOTE: PLEASE NOTIFY DIRECTOR, BENÉT LABORATORIES, ATTN: AMSTA-AR-CCB-O OF ADDRESS CHANGES.

TECHNICAL REPORT EXTERNAL DISTRIBUTION LIST

| | NO. OF COPIES |
|---|---|
| DEFENSE TECHNICAL INFO CENTER<br>ATTN: DTIC-OCA (ACQUISITIONS)<br>8725 JOHN J. KINGMAN ROAD<br>STE 0944<br>FT. BELVOIR, VA 22060-6218 | 2 |
| COMMANDER<br>U.S. ARMY ARDEC<br>ATTN: AMSTA-AR-WEE, BLDG. 3022<br>AMSTA-AR-AET-O, BLDG. 183<br>AMSTA-AR-FSA, BLDG. 61<br>AMSTA-AR-FSX<br>AMSTA-AR-FSA-M, BLDG. 61 SO<br>AMSTA-AR-WEL-TL, BLDG. 59<br>PICATINNY ARSENAL, NJ 07806-5000 | 1<br>1<br>1<br>1<br>1<br>2 |
| DIRECTOR<br>U.S. ARMY RESEARCH LABORATORY<br>ATTN: AMSRL-DD-T, BLDG. 305<br>ABERDEEN PROVING GROUND, MD<br>21005-5066 | 1 |
| DIRECTOR<br>U.S. ARMY RESEARCH LABORATORY<br>ATTN: AMSRL-WM-MB (DR. B. BURNS)<br>ABERDEEN PROVING GROUND, MD<br>21005-5066 | 1 |
| CHIEF<br>COMPOSITES & LIGHTWEIGHT STRUCTURES<br>WEAPONS & MATLS RESEARCH DIRECT<br>U.S. ARMY RESEARCH LABORATORY<br>ATTN: AMSRL-WM-MB (DR. BRUCE FINK)<br>ABERDEEN PROVING GROUND, MD 21005-5066 | 1 |
| COMMANDER<br>U.S. ARMY RESEARCH OFFICE<br>ATTN: TECHNICAL LIBRARIAN<br>P.O. BOX 12211<br>4300 S. MIAMI BOULEVARD<br>RESEARCH TRIANGLE PARK, NC 27709-2211 | 1 |
| COMMANDER<br>ROCK ISLAND ARSENAL<br>ATTN: SIORI-SEM-L<br>ROCK ISLAND, IL 61299-5001 | 1 |
| COMMANDER<br>U.S. ARMY TANK-AUTMV R&D COMMAND<br>ATTN: AMSTA-DDL (TECH LIBRARY)<br>WARREN, MI 48397-5000 | 1 |
| COMMANDER<br>U.S. MILITARY ACADEMY<br>ATTN: DEPT OF CIVIL & MECH ENGR<br>WEST POINT, NY 10966-1792 | 1 |
| U.S. ARMY AVIATION AND MISSILE COM<br>REDSTONE SCIENTIFIC INFO CENTER<br>ATTN: AMSAM-RD-OB-R (DOCUMENTS)<br>REDSTONE ARSENAL, AL 35898-5000 | 2 |
| NATIONAL GROUND INTELLIGENCE CTR<br>ATTN: DRXST-SD<br>2055 BOULDERS ROAD<br>CHARLOTTESVILLE, VA 22911-8318 | 1 |

NOTE: PLEASE NOTIFY COMMANDER, ARMAMENT RESEARCH, DEVELOPMENT, AND ENGINEERING CENTER, BENÉT LABORATORIES, CCAC, U.S. ARMY TANK-AUTOMOTIVE AND ARMAMENTS COMMAND, AMSTA-AR-CCB-O, WATERVLIET, NY 12189-4050 OF ADDRESS CHANGES.

DEPARTMENT OF THE ARMY
ARMAMENT RESEARCH, DEVELOPMENT AND ENGINEERING CENTER
BENÉT LABORATORIES, CCAC
US ARMY TANK-AUTOMOTIVE AND ARMAMENTS COMMAND
WATERVLIET, NY 12189-4000

OFFICIAL BUSINESS
AMSTA-AR-CCB-O
TECHNICAL LIBRARY